Geophysical Research Letters

RESEARCH LETTER
10.1029/2018GL080309

Key Points:
- Colliding streamers can produce electromagnetic radiation in the UHF, SHF, and even higher-frequency range
- Propagating streamers produce insignificant electromagnetic radiation beyond the VHF range
- Under otherwise the same conditions, longer and larger streamers in higher ambient field produce stronger VHF and UHF radiation

Correspondence to:
F. Shi,
Feng.Shi@unh.edu

Citation:
Shi, F., Liu, N., Dwyer, J. R., & Ihaddadene, K. M. A. (2019). VHF and UHF electromagnetic radiation produced by streamers in lightning. *Geophysical Research Letters*, *46*, 443–451. https://doi.org/10.1029/2018GL080309

Received 4 SEP 2018
Accepted 3 DEC 2018
Accepted article online 6 DEC 2018
Published online 10 JAN 2019

VHF and UHF Electromagnetic Radiation Produced by Streamers in Lightning

Feng Shi[1,2], Ningyu Liu[1], Joseph R. Dwyer[1], and Kevin M. A. Ihaddadene[1]

[1]Department of Physics and Space Science Center, University of New Hampshire, Durham, NH, USA, [2]Department of Physics, Auburn University, Auburn, AL, USA

Abstract In this letter, we report simulation results of streamer propagation and collision that produce electromagnetic radiation in the very high frequency (VHF) and ultra high frequency (UHF) bands. The streamers are initiated in overbreakdown field conditions, $1.5E_k$ and $2E_k$, respectively, which may be found during the corona flash stage of negative leader stepping processes. We find that while streamer propagation produces stronger VHF radiation, the head-on collision of streamers dominates UHF, and even higher-frequency radiation. Analysis of the energy spectral densities obtained from different simulation cases shows that the total length and radii of colliding streamers, as well as the ambient field, are important parameters for the UHF radiation produced by streamer collisions. The larger those parameters are, the stronger UHF radiation produced. Finally, by comparing with the measured spectral magnitude of lightning field in the VHF range, it is found that there are probably 10^5–10^7 streamers involved during the lightning corona flash stage.

Plain Language Summary Despite being a familiar phenomenon, the physics of lightning initiation and propagation is not well understood. An effective approach to study lightning is to observe their radio frequency (RF) signals, which is especially critical for understanding the lightning activities inside thunderstorms, because clouds are opaque for other signals. The RF signals with frequencies above about 10 MHz are commonly used to map/image lightning development. They are believed to be produced by the physical process electrically breaking down virgin air. Previous work has shown that electrical breakdown processes known as streamers, which are the precursors of lightning, can produce RF radiation below hundreds of megahertz. Our study investigates a physical process that enables lightning to produce RF radiation above hundreds of megahertz. We find that collisions between streamers can generate rapid increases of electrical current to produce RF emissions extending to tens of gigahertz. The results will be helpful for understanding and interpreting RF observations/measurements of lightning and will generate impact in the field of atmospheric and space electricity.

1. Introduction

Much we have learned about lightning is from the studies of its electromagnetic field (e.g., Le Vine, 1987; Rakov & Uman, 2003; Uman & Krider, 1982). Among those, particular interest has been paid to the radio frequency (RF) emissions in the very high frequency (VHF) band and above, because they contain the information about the electrical breakdown process in lightning and allow for detailed mapping of the lightning development (e.g., Jacobson & Light, 2003; Petersen & Beasley, 2013, 2014; Rakov & Rachidi, 2009; Rison et al., 1999, 2016; Shi et al., 2016; Willett et al., 1990). In particular, over past decades, lightning RF emissions have been used to locate discharge sources and map/image channel development inside thunderclouds (e.g., Krehbiel et al., 1979; Rison et al., 1999; Shao & Krehbiel, 1996; Thomas et al., 2000; Willett et al., 1989). Although it has been suggested that the source of the VHF and ultra high frequency (UHF) emissions appears to be associated with the development of streamers in the breakdown process of lightning (e.g., Brook & Kitagawa, 1964), it is poorly understood how streamer discharges generate these electromagnetic signals. Exponentially growing streamers are found to be able to produce HF and VHF electromagnetic radiation (Shi et al., 2016), but they are not expected to emit strong radiation in UHF and higher-frequency bands, since their growth time constant is on the order of nanoseconds. Consequently, it is necessary to identify other processes that can generate very rapid current variation for producing RF emissions in those frequency bands.

Although not well understood, RF radiation has also been observed from laboratory discharges (e.g., Kim, 2009). It has been found that RF radiation power at ~2.4 GHz is correlated with the emission of X-rays from a long spark (Montanyà et al., 2015). It has been suggested that extremely strong electric field that is required for X-ray production during spark discharges was produced by the head-on collisions of streamers (e.g., Cooray et al., 2009; Kochkin et al., 2012). However, theoretical studies have indicated that the head-on collision of streamers is unlikely to produce significant emissions of X-rays because the enhanced electric field due to collision collapses on a very short timescale of a few picoseconds (Babich & Bochkov, 2017; Ihaddadene & Celestin, 2015; Köhn et al., 2017). The recent work of (Luque, 2017) has shown that streamer collisions are able to produce electromagnetic radiation in the RF spectrum, ranging from tens of megahertz to a few gigahertz at ground pressure at the subbreakdown field conditions.

Streamer collisions, therefore, with their ability to generate current variation on a timescale of picoseconds (e.g., Ihaddadene & Celestin, 2015), may be a significant source for VHF and UHF radiation during the lightning propagation. They are expected to be common in lightning, since during lightning corona flashes, electric field can exceed conventional breakdown threshold field near the leader tip, and negative streamers around the tip of the negative leader may collide with backward-propagating positive streamers initiated from the bidirectional space leaders (e.g., Rakov & Uman, 2003, p.136). Yet no study has been performed to investigate the RF radiation from streamer collisions under the overbreakdown field conditions as far as we know. In addition, microwave emissions at ~1.5 – 1.6 GHz have been observed from lightning (Petersen & Beasley, 2013, 2014). It is thus necessary to investigate how far the RF emissions from streamer collisions extend into the UHF frequency range.

In this letter, we report a study to use simulation results to investigate the RF spectral properties of propagating and colliding streamers at overbreakdown field conditions. It is found that under otherwise the same conditions, propagating streamers dominate the spectrum below ~1 GHz, while colliding streamers dominate the spectrum in the frequency range above. Stronger UHF radiation is emitted if the total length of the colliding streamers or the ambient field is increased.

2. Model

The streamer dynamics is described by drift-diffusion equations for electrons, positive ions, and negative ions, coupled with Poisson's equation in a cylindrically symmetric system. The local field approximation is employed in our model to determine various coefficients, such as the ionization and attachment coefficients, which means the coefficients are assumed to be functions of the local reduced electric field (Liu & Pasko, 2004). The photoionization process producing electron-ion pairs ahead of streamer heads is modeled by using the SP_3 method (Bourdon et al., 2007; Liu et al., 2007). For the results presented in this paper we assume that the ambient electric field is uniform. Simulation results for two ambient field (E_0) cases, $1.5E_k$ and $2E_k$ (with E_k being the conventional breakdown field 3.2×10^6 V/m), are presented below. To initiate two counter-propagating streamers, two spherically symmetric neutral plasma clouds with a peak density (n_0) of 10^{14}cm^{-3} and Gaussian characteristic spatial decay scales (σ_1 and σ_2, respectively) of 0.1 or 0.5 mm are placed with different distances (d_0) from each other at the start of the simulation:

$$n(r,z) = n_0 e^{\left[-\left(\frac{r^2+(z-z_{1,2})^2}{\sigma_{1,2}^2}\right)\right]}, \quad (1)$$

where $z_{1,2}$ denotes the initial position (z_1 or z_2) for each of the plasma clouds, respectively. More detailed description of the model and the employed numerical methods can be found elsewhere (Shi et al., 2016, 2017).

Note that in the model we find the electric field by solving Poisson's equation, instead of solving full Maxwell's equations (Luque, 2017). This is valid because the quasi-electrostatic approximation holds when the light propagation time (δt_c) through the characteristic length scale of the system under study is much smaller than the temporal scale (l) of the process of interest (Δt). According to our simulation results presented below, $l \sim$ 0.1mm (Figure 1b) and $\Delta t \sim$ 10 ps (Figure 1d), thus $\delta t_c \sim$ 0.3ps$\ll\Delta t$, which is on the order of tens of picoseconds. Therefore, the quasi-electrostatic model is still valid and can be used to investigate the head-on collision of streamers.

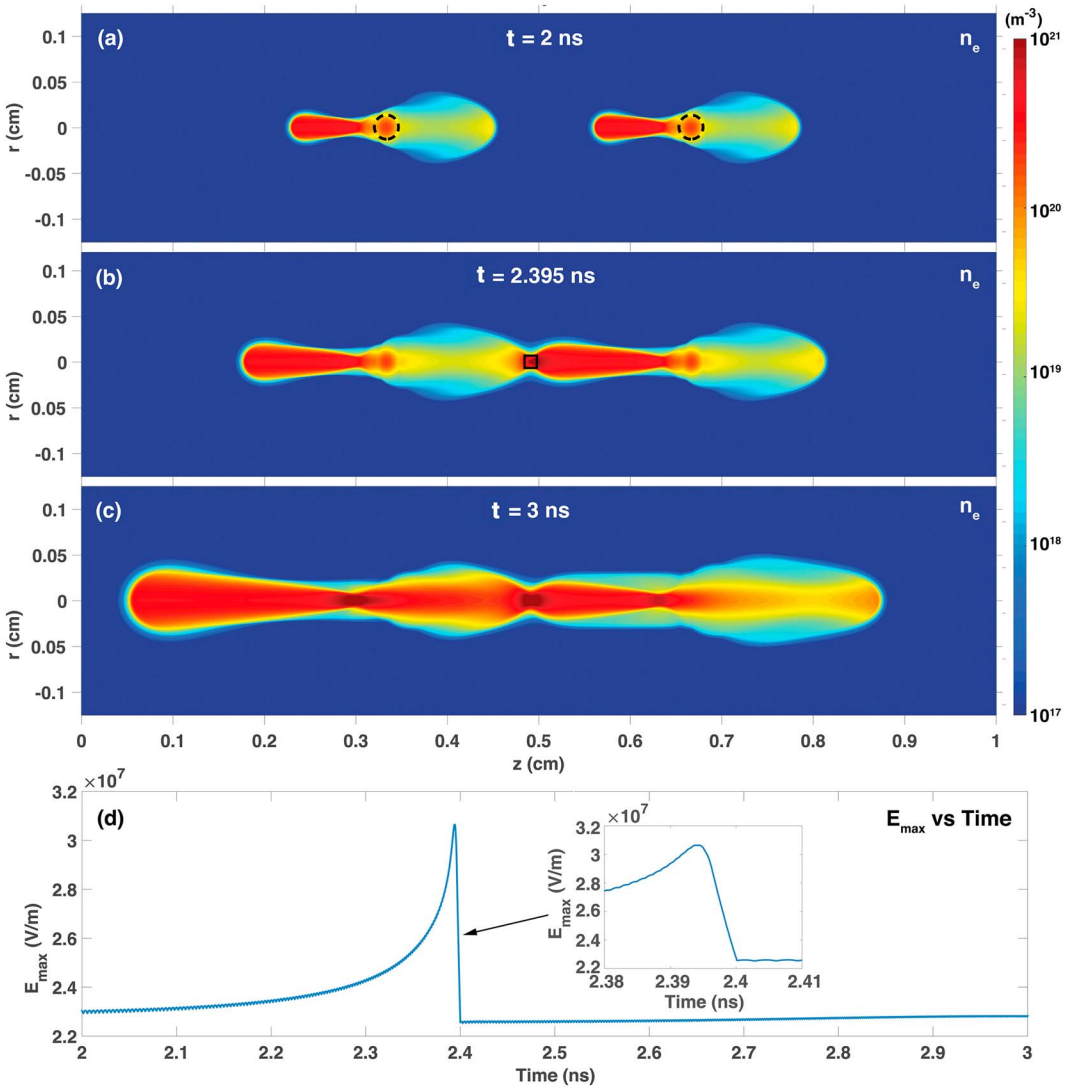

Figure 1. Simulation results for case I (see text). (a) Electron density distribution before collision, showing that two bidirectional propagating streamers have been initiated. (b) Electron density distribution during collision, showing that the electron density is greatly enhanced in the colliding region. (c) Electron density distribution after collision, showing the merging of the two colliding streamers into a single propagating streamer. (d) Maximum electric field as a function of time, showing its increase before collision and its collapse in a very short time interval after collision. Note that ambient electric field points from right to left in (a–c), so that positive streamers propagate to the left side while negative streamers to the right. The black dashed circles in (a) mark the initial patch positions. The black rectangle in (b) shows the colliding region (~0.1 mm). The inset plot in (d) illustrates the timescale (~10 ps) for the collapse of the enhanced field due to collision.

3. Results and Discussion

As shown by previous studies (e.g., Ihaddadene & Celestin, 2015), the magnitude of ambient field is an important factor that determines the maximum field that can be obtained during streamer collision. Because the space charge regions of the two counter-propagating streamers start to neutralize when they are in contact with each other, we expect that their radii are also important factors determining various aspects of streamer collision. This means that the streamer length is important because streamers propagate with expansion and acceleration for the ambient field cases considered here. Four simulation cases are considered in this paper to investigate the properties of the RF radiation from colliding streamers developing in different ambient fields and having different lengths and radii. The values of the simulation setup parameters for the four cases are case I: $d_0 = 0.3$ cm, $\sigma_1 = 0.1$ mm, $\sigma_2 = 0.1$ mm, $E_0 = 1.5E_k$; case II: $d_0 = 1.4$ cm, $\sigma_1 = 0.1$ mm, $\sigma_2 = 0.1$ mm,

$E_0 = 1.5E_k$; case III: $d_0 = 1.4$ cm, $\sigma_1 = 0.1$ mm, $\sigma_2 = 0.5$ mm, $E_0 = 1.5E_k$; and case IV: $d_0 = 0.3$ cm, $\sigma_1 = 0.1$ mm, $\sigma_2 = 0.1$ mm, $E_0 = 2E_k$.

Figures 1a–1c show the electron density distributions before, during and after the head-on collision at three representative moments of time for case I. The initial plasma patches are denoted by black dashed circles in Figure 1a. The ambient electric field ($\boldsymbol{E}_0$) points from right to left, and thus, the left-propagating streamers initiated from the patches are of positive polarity, while those right-propagating streamers are of negative polarity. Figure 1d shows the maximum electric field (E_{max}) in the simulation region as a function of time. At $t = 2$ ns, the electron density distributions of streamers with the same polarity are quite similar, indicating that the interaction between the streamers is negligible before collision, and each bidirectional streamer can be regarded as an isolated propagating streamer. But as the two colliding streamers approach each other, the electric field and thus the ionization rate are enhanced, leading to the increase of electron channel density in the colliding streamers. Encountering streamer fronts thus behave slightly differently from isolated propagating streamers just before the moment of collision, which is consistent with the study of Köhn et al. (2017). The maximum electric field is greatly enhanced (up to $\sim 10E_k$) during the collision but collapses very fast (~10 ps) due to the large increase of the conductivity in the colliding region (Babich & Bochkov, 2017; Ihaddadene & Celestin, 2015; Köhn et al., 2017). After the head-on collision, the two bidirectional streamers merge into one single bidirectional propagating streamer. If no more collision happens afterward, this new bidirectional streamer will propagate similarly as the isolated streamers studied previously (e.g., Shi et al., 2016). In this regard, we can utilize the simulation results from those studies for the properties of the streamer at later stages of its development, such as the growth rate for the streamer acceleration (e.g., Shi et al., 2016).

According to Uman et al. (1975), the magnetic field B_ϕ radiated from an antenna of finite length H can be estimated as

$$B_\phi \sim \frac{\mu_0}{4\pi}\int_0^H \frac{\sin\theta}{cR}\frac{\partial I(z, t - R/c)}{\partial t}\,dz, \tag{2}$$

where θ, c, R, and I are the polar angle, speed of light, distance to the observer, and current flowing in the antenna, respectively. Note that the radiated electric and magnetic fields have the same temporal variation. Assuming that the streamer develops in the vertical direction, giving a vertical current, the radiated magnetic field has B_ϕ component only, which is analyzed to find the spectrum. In particular, if $H \ll R$,

$$B_\phi \propto \frac{\partial}{\partial t}\int_0^H I(z, t - R/c)\,dz \sim \frac{\partial}{\partial t}\left[I_{CM}(t - R/c)\right], \tag{3}$$

where I_{CM} is the current moment. Therefore, in order to obtain the radiated electromagnetic field from the streamer, we need to calculate the time derivative of its current moment. To achieve this, we first need to formulate the current moment waveform from the beginning (initiation) of the streamer to its ending (termination). However, since so far we can only afford to simulate the streamer development in a small high field region that may exist, for example, near the lightning leader tip, the current moment is in the phase of exponential growth. Assuming that a single double-headed streamer is formed after the collision, previous simulation results on exponential growth of streamers in strong electric fields can be used to describe the current moment variation during this phase (Shi et al., 2016).

As the streamer continues to propagate, it will branch or exit the high field region. We have used the three-dimensional streamer code previously developed (Shi et al., 2017) to investigate the current moment variation caused by streamer branching. The results indicate that streamer branching does not lead to rapid changes in the current moment that are required to produce VHF and UHF radiation. As the streamer exits the high field region, it will decay as shown by sprite streamer observations (Li & Cummer, 2009). To model a complete streamer current moment waveform, we use a double exponential function, which is parameterized by our simulation results and sprite streamer observations:

$$I_{CM}(t) = \frac{I_{CM0}\cdot e^{\alpha(t-T_0)}}{1 + e^{(\alpha+\beta)(t-T_0)}}, \tag{4}$$

where I_{CM0}, α, β, and T_0 control the maximum of current moment, the growth rate, the decay rate, and the time when it the current moment reaches the maximum, respectively.

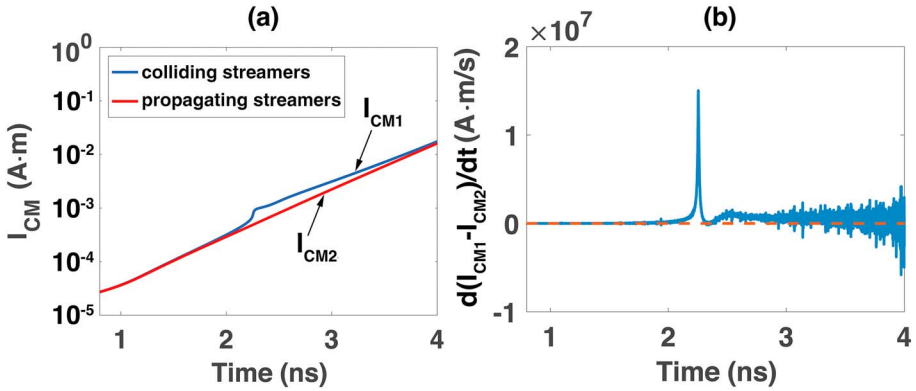

Figure 2. Case I: (a) Current moments for head-on collision streamers (I_{CM1}) and for two isolated propagating streamers (I_{CM2}). (b) The time derivative of the current moment due to the collision, $d(I_{CM1} - I_{CM2})/dt$. The red dashed line shows the zero reference value.

The current moment $I_{CM}(t)$ for case I is shown in Figure 2a, in which the blue curve shows the current moment for the colliding streamers (I_{CM1}) shown in Figure 1, while the red curve for the two isolated propagating streamers (I_{CM2}). It can be seen that before the collision ($t \lesssim 2$ ns), the total current moment shown by the two curves is almost the same. But as the streamers approach and collide with each other, I_{CM1} increases faster than I_{CM2} in a brief time interval. After the collision, the colliding streamers merge into a single bidirectional propagating streamer, so that I_{CM1} and I_{CM2} become almost the same again. In other words, the difference between the two curves results from the head-on collision only, and Figure 2b shows the time derivative of the current moment due to the collision. Given this result, the current moment for the merged streamer formed after the collision can be expected to grow exponentially with the same growth rate as the isolated bidirectional propagating streamers previously studied (e.g., Liu & Pasko, 2004; Shi et al., 2016).

On the other hand, it is a natural consequence that the current moment will grow slower and then decay eventually. The decay is modeled as an exponential process in equation (4). The decay rate of the current moment is assumed to be three times of that of streamer deceleration, just as the growth rate of current moment (e.g., $\sim 1.7\times10^9$ s^{-1} for case I) being three times of streamer acceleration (e.g., $\sim 6\times10^8$ s^{-1} for case I; Shi et al., 2016). From the observation of decelerating sprite streamers (Li & Cummer, 2009), the range of the current moment decay rate for decaying streamers can be estimated as $\sim 6\times10^6 - 7\times10^7$ s^{-1} at ground pressure according to similarity laws (e.g., Kosar et al., 2012; Liu & Pasko, 2004). We further assume the transition between growth and decay occurs when the propagating streamer reaches the maximum speed $\sim 5\times10^7$ m/s observed for sprite streamers (e.g., Liu et al., 2015; McHarg et al., 2007) or narrow bipolar events (e.g., Rison et al., 2016).

As an example, the current moment for case I shown in Figure 3a is obtained with $\alpha = 1.7\times10^9 s^{-1}$, $\beta = 7.5\times10^7 s^{-1}$, $I_{CM0} = 0.44$ A·m, and $T_0 = 6$ ns when propagating streamers are assumed in transition to decay at the speed of $\sim 5\times10^7$ m/s. The asymmetric bipolar shape of dI_{CM}/dt in Figure 3b, with a sharper and larger positive peak, results from the rapid growth and relatively slow decay of the current moment. Also note that the change of the current moment and its time derivative due to collision is shown in the insets of Figure 3.

In order to obtain the electromagnetic radiation spectrum, we need to perform Fourier analysis of dI_{CM}/dt, which can be expressed as

$$\left| F\left[\frac{dI_{CM}(t)}{dt}\right]\right| = \omega \cdot \left|\tilde{I}_{CM}(\omega)\right|, \tag{5}$$

where ω is the angular frequency. The Fourier transform of $d\left(I_{CM1} - I_{CM2}\right)/dt$ due to collision in Figure 2b is shown by the green line in Figure 4a. We can clearly see that due to the short timescale of the pulse, the radiation frequency spans the UHF range and extends to SHF and even higher-frequency bands. Note that because of the short time window used in the Fourier analysis (e.g., 1–3 ns in case I), the resolution for the spectrum in Figure 2b is 0.5 GHz.

Now let us consider the Fourier analysis of the I_{CM} model described by equation (4). With the parameters $\alpha = 1.7\times10^9 s^{-1}$, $\beta_1 = 7.5\times10^7 s^{-1}$, $I_{CM0} = 0.44$ A·m, and $T_0 = 6$ ns (see Figure 3a), the frequency spectrum is shown by the blue curve in Figure 4a. With otherwise the same parameters, the red curve corresponds to a

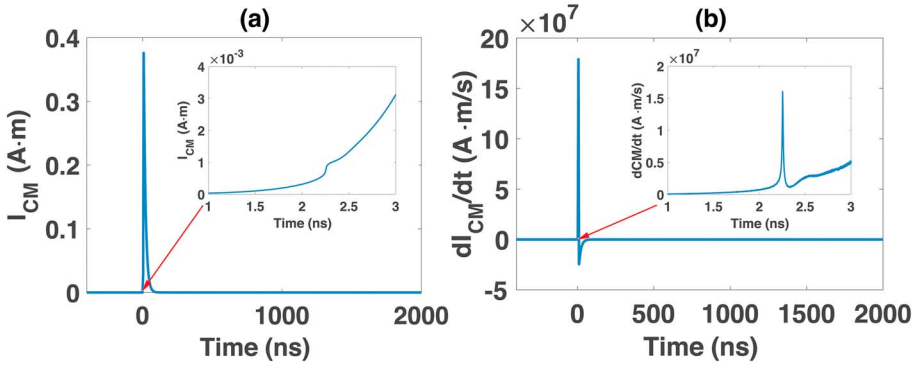

Figure 3. Case I: (a) Model I_{CM}, obtained by using equation (4) with $\alpha = 1.7 \times 10^9 s^{-1}$, $\beta = 7.5 \times 10^7 s^{-1}$, and $I_{CM0} = 0.4$ A·m. The inset plot shows the detailed profile during 1–3 ns. (b) The corresponding dI_{CM}/dt. The inset plot shows the detailed profile during 1–3 ns.

slower decay in I_{CM} (with $\beta_2 = 6 \times 10^6 s^{-1}$), the yellow corresponds to a larger $T_0 = 7$ ns (with $I_{CM0} = 2.3$ A·m assuming the same growth rate), and the purple corresponds to two isolated propagating streamers without collision shown by the red line in Figure 2a. It is clearly shown that the UHF (up to ~3 GHz), SHF (up to ~30 GHz) and even higher-frequency radiation is dominated by the collision process, not by the propagation process. Moreover, Figure 4 shows that β or T_0 hardly affects the radiation above ~1 GHz. In other words, even if there is a large uncertainty in their values, the results on UHF radiation above ~1 GHz vary negligibly. The figure thus indicates that the radiation above ~1 GHz is predominantly produced by streamer collision. Also note that for the VHF emissions produced by propagating streamers, Qin et al. (2012) found streamers can produce electromagnetic radiation up to ~0.3 MHz at 40-km altitude, which is consistent with the results shown in Figure 4a when scaling to ground level (~0.1 GHz) using similarity laws.

Knowing the electromagnetic radiation spectrum, we can estimate the energy radiated in the VHF and UHF bands. According to the antenna model, $E(\omega) = [\sin\theta/(4\pi\varepsilon_0 c^2 R)](\omega \tilde{I}_{CM})$ (Uman, 2001, A.3.4), and the Poynting vector $S(\omega) = c\varepsilon_0 |\tilde{E}(\omega)|^2$. The energy spectral density (ESD) in Fourier space thus can be expressed as $P(\omega) = \int_\Omega S(\omega) \cdot R^2 d\Omega = [1/(6\pi\varepsilon_0 c^3)](\omega \tilde{I}_{CM})^2$. Therefore, the total energy in a given frequency band (ω_1, ω_2) can be evaluated as

$$W = 2\int_{\omega_1}^{\omega_2} P(\omega)\, d\omega = \int_{\omega_1}^{\omega_2} \frac{1}{3\pi\varepsilon_0 c^3} \left(\omega \tilde{I}_{CM}\right)^2 d\omega, \tag{6}$$

where a factor of 2 means that negative frequency components are treated equally as their positive counterparts.

Figure 4b shows the ESD spectra for all four simulation cases. It can be seen that for the same ambient field of $1.5E_k$, as the combined length of the head-on collision streamers increases (see 0.3 cm in case I and 1.4 cm in case II), the radiated energy in the VHF range increases by approximately five times, while the UHF energy increases by ~7,500 times. However, if the radius of one of the head-on collision streamers is increased (see cases II and III), the radiated energy in the VHF range becomes larger (~6 times), but the UHF energy content does not change too much. Also note that the ambient field plays an important role in the radiated energy spectrum. When the ambient field is increased from $1.5E_k$ to $2E_k$ (i.e., cases I and IV), the radiated energy spectrum is shifted toward the higher frequency, indicating that the radiation due to streamer collision takes over the spectrum at a higher frequency.

Finally, if the measurements of the VHF and UHF spectral magnitude of electromagnetic radiation from lightning are available, the number of streamers or streamer collisions required to generate the observed field may be estimated by using the results presented in Figure 4b, with the assumption of each streamer experiencing one collision. According to observations of lightning radiation (e.g., Le Boulch et al., 1987), the amplitude of electric field spectral density in VHF range is on the order of $\sim 3 \times 10^{-9}$ V/m/Hz at 10-km altitude, and thus, the radiation energy in the VHF band can be estimated at $\sim 1 \times 10^{-2}$ J. According to our simulation of case I, the VHF radiation energy is $\sim 10^{-8}$ J, so $\sim 10^6$ streamers are needed to produce the measured VHF radiation energy. In this scenario, the UHF radiation energy would be $\sim 10^{-7}$ J. Similarly, with the same assumption for cases II, III and IV, the required numbers of streamers are $\sim 3.5 \times 10^5$, $\sim 5 \times 10^4$ and $\sim 2.5 \times 10^6$, respectively, and thus the UHF radiation energy would be $\sim 3 \times 10^{-4}$ J, $\sim 1 \times 10^{-5}$ J, and $\sim 2 \times 10^{-5}$ J, respectively. Note that

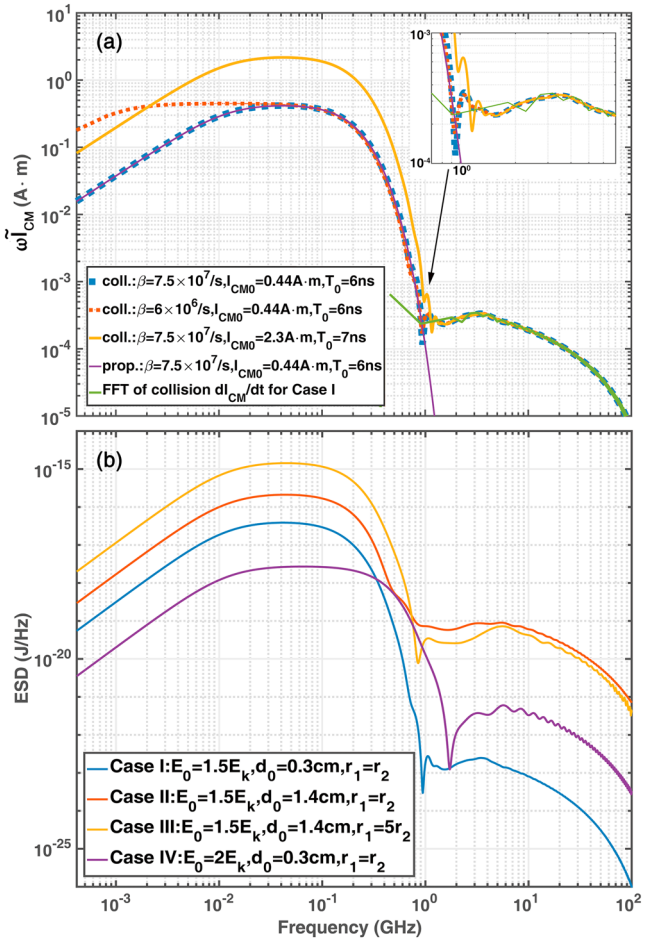

Figure 4. (a) The frequency spectrum obtained from the I_{CM} model described by equation (4) with different parameters, as well as from simulation results, for case I. Specifically, the blue curve corresponds to the parameters: $\alpha = 1.7 \times 10^9 s^{-1}$, $\beta = 7.5 \times 10^7 s^{-1}$, $I_{CM0} = 0.44$ A·m, and $T_0 = 6$ ns. With otherwise the same parameters, the red curve corresponds to $\beta = 6 \times 10^6 s^{-1}$, and the yellow shows results for $T_0 = 7$ ns and $I_{CM0} = 2.3$ A·m. The purple shows the results for two isolated propagating streamers, that is, without the change of I_{CM} due to collision, as shown by the red curve in Figure 2a. The green shows fast Fourier transform results of collision signals (see Figure 2b) during 1–3 ns. Note that the dI_{CM}/dt spectrum above the UHF range for colliding streamers almost overlap (zoomed-in view by the inset plot) regardless of the modeling parameters, while for propagating streamers it decays very fast and produces noise that cannot be resolved by the analysis. (b) The energy spectral density for all four simulation cases.

from the electrostatic consideration of the streamer zone (e.g., Celestin et al., 2015), 10^5–10^7 streamers are required to give a potential drop of 2–20 MV near the lightning leader tip, which is commonly accepted for typical lightning leaders and also consistent with analysis of ground-based observation of X-rays produced by lightning (e.g., Xu et al., 2014).

4. Conclusions

The electromagnetic radiation due to head-on collision of streamers under overbreakdown field conditions is investigated. It is shown that the head-on collisions of streamers near the lightning leader tip, particularly during the corona flash stage of a stepped leader, can be an important source of UHF, SHF, or even higher-frequency radiation. In contrast, propagating streamers produce insignificant electromagnetic radiation in those frequencies but are dominant sources of VHF radiation. The magnitude and duration of the brief current pulse generated by the head-on collision depend on the ambient field and total length of the two colliding streamers. The ESD obtained from Fourier analysis indicates that the longer the streamer length is or the larger the streamer radii are, the stronger the radiation is. If the ambient field is larger, the radiation is also stronger. A comparison of the modeling results with the measured spectral magnitude of the lightning electromagnetic field in the VHF range shows that there are probably a total of ~10^5–10^7 streamers involved.

Acknowledgments
This work was supported in part by the National Science Foundation Grant AGS-1348046 and the Air Force Office of Scientific Research under award FA9550-18-1-0358 to the University of New Hampshire. Simulation data allowing to reproduce our figures are available from https://figshare.com/s/278992d9163767de7d0a.

References

Babich, L., & Bochkov, E. (2017). Numerical simulation of electric field enhancement at the contact of positive and negative streamers in relation to the problem of runaway electron generation in lightning and in long laboratory sparks. *Journal of Physics D: Applied Physics*, *50*(45), 455202.

Bourdon, A., Pasko, V. P., Liu, N. Y., Célestin, S., Ségur, P., & Marode, E. (2007). Efficient models for photoionization produced by non-thermal gas discharges in air based on radiative transfer and the Helmholtz equations. *Plasma Sources Science and Technology*, *16*, 656–678. https://doi.org/10.1088/0963-0252/16/3/026

Brook, M., & Kitagawa, N. (1964). Radiation from lightning discharges in the frequency range 400 to 1000 Mc/s. *Journal of Geophysical Research*, *69*(12), 2431–2434.

Celestin, S., Xu, W., & Pasko, V. P. (2015). Variability in fluence and spectrum of high-energy photon bursts produced by lightning leaders. *Journal of Geophysical Research: Space Physics*, *120*, 10,712–10,723. https://doi.org/10.1002/2015JA021410

Cooray, V., Arevalo, L., Rahman, M., Dwyer, J., & Rassoul, H. (2009). On the possible origin of X-rays in long laboratory sparks. *Journal of Atmospheric and Solar-Terrestrial Physics*, *71*(17-18), 1890–1898. https://doi.org/10.1016/j.jastp.2009.07.010

Ihaddadene, M. A., & Celestin, S. (2015). Increase of the electric field in head-on collisions between negative and positive streamers. *Geophysical Research Letters*, *42*, 5644–5651. https://doi.org/10.1002/2015GL064623

Jacobson, A. R., & Light, T. E. L. (2003). Bimodal radio frequency pulse distribution of intracloud-lightning signals recorded by the FORTE satellite. *Journal of Geophysical Research*, *108*(D9), 4266. https://doi.org/10.1029/2002JD002613

Kim, C. J. (2009). Electromagnetic radiation behavior of low-voltage arcing fault. *IEEE transactions on power delivery*, *24*(1), 416–423. https://doi.org/10.1109/TPWRD.2008.2002873

Kochkin, P. O., Nguyen, C. V., van Deursen, A. P., & Ebert, U. (2012). Experimental study of hard X-rays emitted from metre-scale positive discharges in air. *Journal of Physics D: Applied Physics*, *45*(42), 425202.

Köhn, C., Chanrion, O., & Neubert, T. (2017). Electron acceleration during streamer collisions in air. *Geophysical Research Letters*, *44*, 2604–2613. https://doi.org/10.1002/2016GL072216

Kosar, B. C., Liu, N. Y., & Rassoul, H. K. (2012). Luminosity and propagation characteristics of sprite streamers initiated from small ionospheric disturbances at subbreakdown conditions. *Journal of Geophysical Research*, *117*, A08328. https://doi.org/10.1029/2012JA017632

Krehbiel, P. R., Brook, M., & McCrory, R. A. (1979). An analysis of the charge structure of lightning discharges to ground. *Journal of Geophysical Research*, *84*(NC5), 2432–2456.

Le Boulch, M., Hamelin, J., & Weidman, C. (1987). UHF-VHF radiation from lightning. *Electromagnetics*, *7*(3-4), 287–331.

Le Vine, D. M. (1987). Review of measurements of the RF spectrum of radiation from lightning. *Meteorology and Atmospheric Physics*, *37*(3), 195–204.

Li, J., & Cummer, S. A. (2009). Measurement of sprite streamer acceleration and deceleration. *Geophysical Research Letters*, *36*, L10812. https://doi.org/10.1029/2009GL037581

Liu, N. Y., Célestin, S., Bourdon, A., Pasko, V. P., Ségur, P., & Marode, E. (2007). Application of photoionization models based on radiative transfer and the Helmholtz equations to studies of streamers in weak electric fields. *Applied Physics Letters*, *91*(211501). https://doi.org/10.1063/1.2816906

Liu, N. Y., Dwyer, J. R., Stenbaek-Nielsen, H. C., & McHarg, M. G. (2015). Sprite streamer initiation from natural mesospheric structures. *Nature of Communications*, *6*, 7540. https://doi.org/10.1038/ncomms8540

Liu, N. Y., & Pasko, V. P. (2004). Effects of photoionization on propagation and branching of positive and negative streamers in sprites. *Journal of Geophysical Research*, *109*, A04301. https://doi.org/10.1029/2003JA010064

Luque, A. (2017). Radio frequency electromagnetic radiation from streamer collisions. *Journal of Geophysical Research: Atmospheres*, *122*, 10,497–10,509. https://doi.org/10.1002/2017JD027157

McHarg, M. G., Stenbaek-Nielsen, H. C., & Kammae, T. (2007). Observations of streamer formation in sprites. *Geophysical Research Letters*, *34*, L06804. https://doi.org/10.1029/2006GL027854

Montanyà, J., Fabró, F., March, V., van der Velde, O., Solà, G., Romero, D., & Argemí, O. (2015). X-rays and microwave RF power from high voltage laboratory sparks. *Journal of Atmospheric and Solar-Terrestrial Physics*, *136*, 94–97.

Petersen, D. A., & Beasley, W. H. (2013). High-speed video observations of a natural negative stepped leader and subsequent dart-stepped leader. *Journal of Geophysical Research: Atmospheres*, *118*, 12,110–12,119. https://doi.org/10.1002/2013JD019910

Petersen, D., & Beasley, W. (2014). Microwave radio emissions of negative cloud-to-ground lightning flashes. *Atmospheric Research*, *135*, 314–321.

Qin, J., Celestin, S., & Pasko, V. P. (2012). Low frequency electromagnetic radiation from sprite streamers. *Geophysical Research Letters*, *39*, L22803. https://doi.org/10.1029/2012GL053991

Rakov, V. A., & Rachidi, F. (2009). Overview of recent progress in lightning research and lightning protection. *IEEE Transactions on Electromagnetic Compatibility*, *51*(3), 428–442.

Rakov, V. A., & Uman, M. A. (2003). *Lightning: Physics and effects*. Cambridge, UK and New York: Cambridge University Press.

Rison, W., Krehbiel, P. R., Stock, M. G., Edens, H. E., Shao, X.-M., Thomas, R. J., et al. (2016). Observations of narrow bipolar events reveal how lightning is initiated in thunderstorms. *Nature Communications*, *7*, 10721. https://doi.org/10.1038/ncomms10721

Rison, W., Thomas, R. J., Krehbiel, P. R., Hamlin, T., & Harlin, J. (1999). A GPS-based three-dimensional lightning mapping system: Initial observations in central New Mexico. *Geophysical Research Letters*, *26*(23), 3573–3576. https://doi.org/10.1029/1999GL010856

Shao, X. M., & Krehbiel, P. R. (1996). The spatial and temporal development of intracloud lightning. *Journal of Geophysical Research*, *101*(D21), 26,641–26,668.

Shi, F., Liu, N. Y., & Dwyer, J. R. (2017). Three-dimensional modeling of two interacting streamers. *Journal of Geophysical Research: Atmospheres*, *122*, 10,169–10,176. https://doi.org/10.1002/2017JD026935

Shi, F., Liu, N. Y., & Rassoul, H. K. (2016). Properties of relatively long streamers initiated from an isolated hydrometeor. *Journal of Geophysical Research: Atmospheres*, *121*, 7284–7295. https://doi.org/10.1002/2015JD024580

Thomas, R. J., Krehbiel, P. R., Rison, W., Hamlin, T., Boccippio, D. J., Goodman, S. J., & Christian, H. J. (2000). Comparison of ground-based 3-dimensional lightning mapping observations with satellite-based LIS observations in Oklahoma. *Geophysical Research Letters*, *27*(12), 1703–1706. https://doi.org/10.1029/1999GL010845

Uman, M. A. (2001). *The Lightning Discharge*. Mineola, New York: Dover. unabridged ed.

Uman, M. A., & Krider, E. P. (1982). A review of natural lightning: Experimental data and modeling. *IEEE Transactions on Electromagnetic Compatibility*, *EMC-24*(2), 79–112.

Uman, M. A., McLain, D. K., & Krider, E. P. (1975). The electromagnetic radiation from a finite antenna. *American Journal of Physical*, *43*, 33–38. https://doi.org/10.1119/1.10027

Willett, J. C., Bailey, J. C., & Krider, E. P. (1989). A class of unusual lightning electric field waveforms with very strong high-frequency radiation. *Journal of Geophysical Research*, *94*, 16,255–16,267. https://doi.org/10.1029/JD094iD13p16255

Willett, J. C., Bailey, J. C., Leteinturier, C., & Krider, E. P. (1990). Lightning electromagnetic radiation field spectra in the interval from 0.2 to 20 MHz. *Journal of Geophysical Research*, *95*, 20,367–20,387. https://doi.org/10.1029/JD095iD12p20367

Xu, W., Celestin, S., & Pasko, V. P. (2014). Modeling of X-ray emissions produced by stepping lightning leaders. *Geophysical Research Letters*, *41*, 7406–7412. https://doi.org/10.1002/2014GL061163